Helical Lévy walks: Adjusting searching statistics to resource availability in microzooplankton

Frederic Bartumeus*†‡, Francesc Peters§, Salvador Pueyo*, Cèlia Marrasé§, and Jordi Catalan†

*Departament d'Ecologia, Universitat de Barcelona, Avinguda Diagonal 645, 08028 Barcelona, Catalonia, Spain; §Institut de Ciències del Mar, Centre Mediterrani d'Investigacions Marines i Ambientals (Consejo Superior de Investigaciones Científicas), Passeig Marítim de la Barceloneta, 37-49, 08003 Barcelona, Catalonia, Spain; and †Centre d'Estudis Avançats de Blanes, Consejo Superior de Investigaciones Científicas, Accés Cala Sant Francesc, 14, 17300 Blanes, Catalonia, Spain

Edited by Simon A. Levin, Princeton University, Princeton, NJ, and approved August 22, 2003 (received for review November 27, 2002)

The searching trajectories of different animals can be described with a broad class of flight length (l_j) distributions with $P(l_j) = l_j^{-\mu}$. Theoretical studies have shown that changes in these distributions (i.e., different μ values) are key to optimizing the long-term encounter statistics under certain searcher–resource scenarios. In particular, they predict the advantage of Lévy searching ($\mu \approx 2$) over Brownian motion ($\mu \geq 3$) for low-prey-density scenarios. Here, we present experimental evidence of predicted optimal changes in the flight-time distribution of a predator's walk in response to gradual density changes of its moving prey. Flight times of the dinoflagellate *Oxyrrhis marina* switched from an exponential to an inverse square power-law distribution when the prey (*Rhodomonas* sp.) decreased in abundance. Concomitantly, amplitude and frequency of the short-term helical path increased. The specific biological mechanisms involved in these searching behavioral changes are discussed. We suggest that, in a three-dimensional environment, a stronger helical component combined with a Lévy walk searching strategy enhances predator's encounter rates. Our results support the idea of universality of the statistical laws in optimal searching processes despite variations in the biological details of the organisms.

Random walks based on Lévy flight distributions $P(l_j) = l_j^{-\mu}$ in concrete "Lévy walks" with $\mu \approx 2$, are the optimal searching strategy for scarce fixed targets that are randomly located (1). A Lévy walk could be more efficient than the usual Gaussian (i.e., Brownian) motion as suggested by early works on microzooplankton (2–4), although Brownian motion is generally assumed in reaction-diffusion predator–prey models. Recently, ecological examples of Lévy walks have been provided for a wide range of animal species (5–10). However, the theoretical study of more complex scenarios has shown that the advantage of Lévy searching over other types of motion is restricted to a set of prey densities, and mobility and size of the predator relative to the prey (11–13). Therefore, natural selection should favor flexible behaviors, combining different searching strategies (i.e., searching statistics) under different conditions. Here, we present experimental evidence that changes occur in both the short- and long-term searching statistics of a predator (*Oxyrrhis marina*), coinciding with density changes of its moving prey (*Rhodomonas* sp.). The specific biological mechanisms involved are also identified.

The marine heterotrophic dinoflagellate *O. marina* has two flagella, one transversal and one longitudinal, providing three types of movement: rotation, translation, and sudden directional changes (14, 15). The flagellar apparatus of *O. marina* has been well studied at both the cellular (15) and the ultrastructural (16) level. Continuous flagellar movements are responsible for simultaneous rotation and translation of organisms, giving rise to a helical path during movement. Normal helical motion is interrupted by sudden (60–100 ms) changes in direction in response to direct, local mechanical stimuli, the so-called "avoidance reactions." However, this term does not embrace the wide variety of conditions under which this behavior is observed. Thus, the term "reorientation leaps" is preferred. Reorientation leaps in *O. marina* are generated by transient arrests of the longitudinal flagellum beat. These leaps are accompanied by a switch from a backward to forward orientation (see figure 5 in ref. 15). Videotape observations of *O. marina* movements show that the helical path is usually straight with occasional smooth, albeit significant, changes in trajectory. These changes are due to momentary changes in the amplitude and frequency of the gyres in the helical path. Despite this feature, the most efficient changes in trajectory are caused by the reorientation leaps. These specific and discrete reactions govern the long-term searching walk in *O. marina*.

To test the hypothesis that changes in the long-term searching behavior of *O. marina* occur as a response to resource availability, two independent experiments were performed by using culture innocula of *O. marina* at two different times of the year.

Methods

Experimental Organisms and Design. In both experiments, the dinoflagellate was grown in a 1-liter container under controlled temperature and light conditions with the smaller autotrophic flagellate *Rhodomonas* sp. as food source. Live samples were withdrawn at 24- or 48-h intervals and immediately videotaped for 2 weeks in experiment A, and for 1 week in experiment B. The two experiments were carried out several months apart and are considered replicate experiments. The movement of *O. marina* in a Palmer cell was videotaped by using a charge-coupled device camera attached to a stereomicroscope immediately after withdrawal from incubation containers. Also, samples were fixed with Lugol's solution for cell enumeration. Prey and predators ranged from 10^1 to 10^5 individuals per ml; predators increasing and prey decreasing through time in the two experiments. Random digital movies of 150 frames (12 frames per s in experiment A, and 8 frames per s in experiment B) were taken from the complete videofilm. The cell 2D positions (Fig. 1) were analyzed by using the NIH IMAGE ANALYSIS software (National Institutes of Health, http://rsb.info.nih.gov/nih-image). Trajectories, swimming velocities, and successive tumbling angles were determined.

Data Analysis. The experimental data set comprised individual trajectory series for *O. marina* with a sampling length ranging from 10 to 180 walk steps, with usual values of ≈50. Data in each of the experiments were grouped into three prey-density ranges, covering the three main resource scenarios, i.e., conditions typical of blooms (1×10^4 to 1×10^5 cells per ml), productive areas ($1–2 \times 10^3$ cells per ml), and open ocean (1×10^1 to 5×10^2 cells per ml). Included in the analyses were 192 and 372 individual positions and tumbling angle series for experiments A and B, respectively. Velocity estimates of *O. marina* were

This paper was submitted directly (Track II) to the PNAS office.

Abbreviations: HFR, high-frequency regime; LFR, low-frequency regime.

‡To whom correspondence should be addressed. E-mail: fbartu@ceab.csic.es.

ECOLOGY

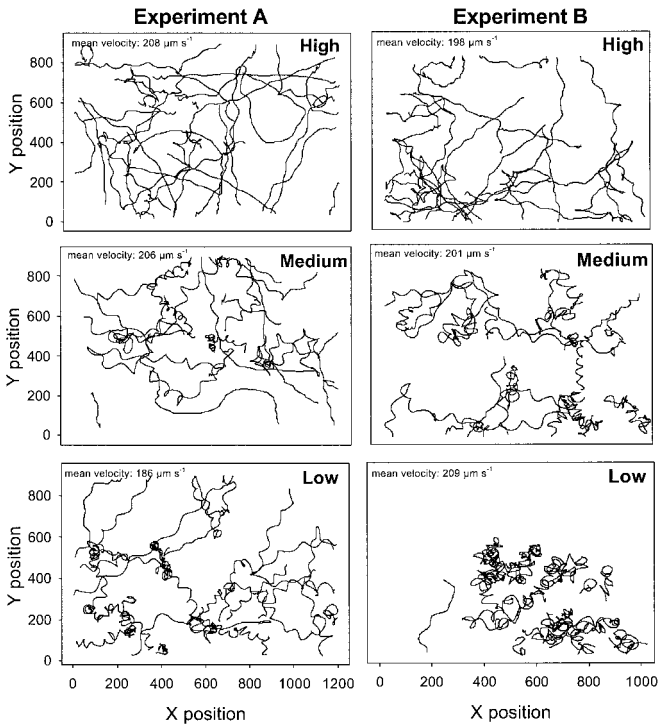

Fig. 1. Representative 2D cell trajectories of *O. marina* in experiments A and B with various densities of *Rhodomonas* sp. prey: high (1×10^4 to 1×10^5 cells per ml), medium ($1–2 \times 10^3$ cells per ml), and low (1×10^1 to 5×10^2 cells per ml). The sampling effort has been fixed (i.e., the same number of walk steps in each resource scenario) to clarify the general searching pattern. An increase in the helical path as resources decrease is observed. At the scale of observation, Lévy walks visually result in a combination of short-walk clusters with long travels between them, whereas Brownian walks look more like straight paths with crossover. Thus, Brownian walkers cover the space more homogeneously than Lévy walkers do.

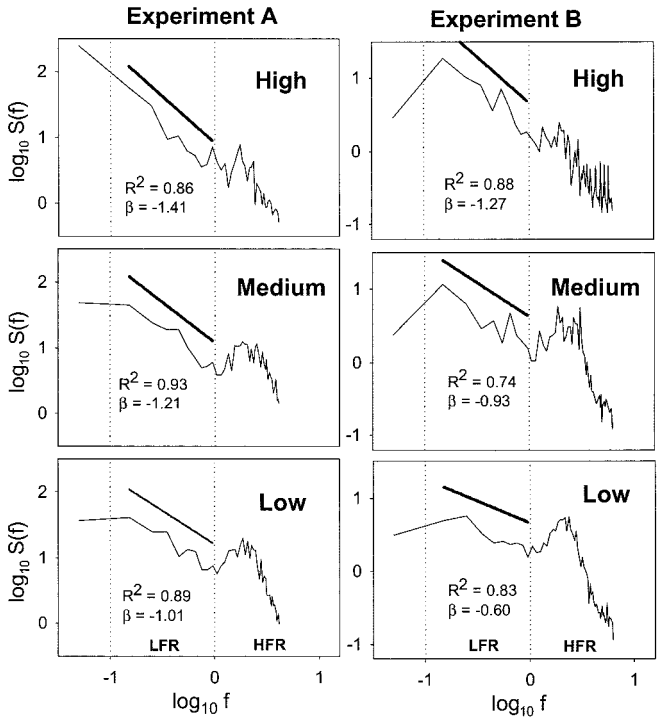

Fig. 2. Log–log plots of the sum of power spectra [$S(f)$] against frequency (f), in hertz, in both experiments and each resource scenario. Vertical dotted lines distinguish two frequency regimes: (*i*) a HFR ($\log f > 0$) and a LFR ($\log f < 0$). A marked periodical signal at HFR (≈2 Hz) was observed with decreasing resources. At the LFR we defined the scaling exponent β by $S(f) \approx f^{-\beta}$; the least-square fittings are indicated by straight lines transposed upward for clarity, although the narrow range of the LFR makes the scaling questionable (see *Results*).

computed for each individual series as the Euclidean distance between successive 2D positions. Mean velocities were computed for data series in each of the three prey-density ranges.

x velocity fluctuation series were obtained by computing changes in x coordinate positions. A power spectrum analysis (17) was performed on each series. Spectra were averaged for all time series in each resource scenario and binned at 0.1 frequency intervals (see Fig. 2). We also computed, for each resource scenario, (*i*) the distribution of tumbling angles, measured as changes in direction at fixed time steps (≈0.1 s) and scaled from 0 to 180° (see Fig. 3) and, (*ii*) the distribution of flight-time intervals, the periods of time between changes in direction (18–20). The distribution of flight times in each of the three resource scenarios (see Fig. 4) was taken as indicative of the average individual behavior. The individual and averaged spectra of velocity fluctuations were similar, giving support to this assumption.

Results

Velocity Fluctuations. Mean velocities (computed as the Euclidean distances between two successive 2D positions) were ≈200 $\mu m \cdot s^{-1}$. Standard deviations ranged from 93.18 to 128.58 $\mu m \cdot s^{-1}$. No clear pattern of change of mean velocity was identified with decreases in resource availability. Therefore, swimming patterns were not related to changes in mean velocity in experiments (Fig. 1).

The spectral analysis based on continuous x velocity fluctuations showed both helical path and reorientation leaps of *O. marina*. A high-frequency regime (HFR) and a low-frequency regime (LFR) were distinguishable in each spectrum (Fig. 2). HFR reflects the short-term changes, which include the helical path, whereas LFR reflects the long-term searching behavior and, thus, the reorientation leap statistics. As resources became scarce, a gradual and significant increase of a periodical signal was observed at ≈2 Hz (HFR). This periodical signal increased in both frequency and amplitude [i.e., mean $S(f)$ value and mean maximum $S(f)$ value ranging from 1 to 3 Hz, Table 1]. The LFR of the spectra seemed to indicate a "$1/f$ noise" [$S(f) \approx f^{\beta}$, $\beta \approx -1$] scaling persistence (17, 21, 22), which decreased (lower LFR slopes) with decreasing resources. However, the influence of the periodical signal and the shortness of the series make the interpretation of the LFR scaling questionable. Indeed, any nonscaling spectra could be approximated to a scaling spectrum at sufficiently narrow frequency ranges. Results were the same for y velocity-transformed series spectra, suggesting isometric conditions occurred during the experiment. Moreover, spectra of individual time series showed the same trends and similar periodical signal variances as the averaged series, indicating that the amalgamated population series that were analyzed reflected individual behaviors.

Tumbling Angles. The frequency distributions of tumbling angles as resources decreased (Fig. 3) showed a relative increase in intermediate-angle classes as compared with in low angle classes, particularly when resources changed from high to medium concentrations. In contrast, the distribution tails (large angles) were mostly uniform for the three resource scenarios. The angle class dividing the two histogram regions of contrasting response was the same for the three conditions (Fig. 3). The helical path involved mainly small tumbling angles: the larger the angle, the

Table 1. Monte Carlo randomization tests (n = 1,000) for mean $S(f)$ value and mean maximum $S(f)$ frequency changes in the HFR periodical signal ranging from 1 to 3 Hz at different resource concentration scenarios

	Experiment A		Experiment B		Experiment A		Experiment B	
Resource comparison	Mean $S(f)$	P	Mean $S(f)$	P	Mean maximum frequencies	P	Mean maximum frequencies	P
High vs. low	2.68 vs. 11.48	0.000	1.59 vs. 3.55	0.000	1.69 vs. 1.96	0.004	1.87 vs. 1.91	0.562
High vs. medium	2.68 vs. 8.15	0.000	1.59 vs. 3.19	0.000	1.69 vs. 1.99	0.004	1.87 vs. 1.99	0.185
Medium vs. low	8.15 vs. 11.48	0.007	3.19 vs. 3.55	0.341	1.99 vs. 1.96	0.740	1.99 vs. 1.91	0.248

lower was its frequency, whereas reorientation leaps due to flagellar strokes usually caused strong cell reorientations (large tumbling angles). Therefore, based on data (Fig. 3), we chose 100° as the cut-off angle between helical paths and reorientation leaps. The latter govern the long-term searching walk and, thus, can be considered as the effective tumbling angles. If effective directions were taken entirely at random, one would expect the mean angular deviation to be 90°. Deviations caused by active flagellar reorientation of cells have also been observed in other microorganisms, such as *Escherichia coli*, with an average (effective) tumbling angle of 103° (23).

To improve the analysis of the long-scale component (i.e., for studying the macroscopic diffusion patterns), it might be desirable to subtract the helical path signal. Crenshaw and coauthors (24) have appropriately characterized 3D helical tracks by means of the finite-helix-fit technique. However, even with a good description of the helical path, it is not straightforward to subtract the helicoid from the original trajectories of a number of individuals without significantly compromising the reliability of the long-term walk statistics. In the future, more accurate approaches for separating the two scale components may improve the characterization and understanding of the long-term searching behavior of microzooplankton. Nevertheless, our method (i.e., looking at the distribution of the tumbling angles), despite its crudeness, is sufficient to preserve the long-term signature of the walk.

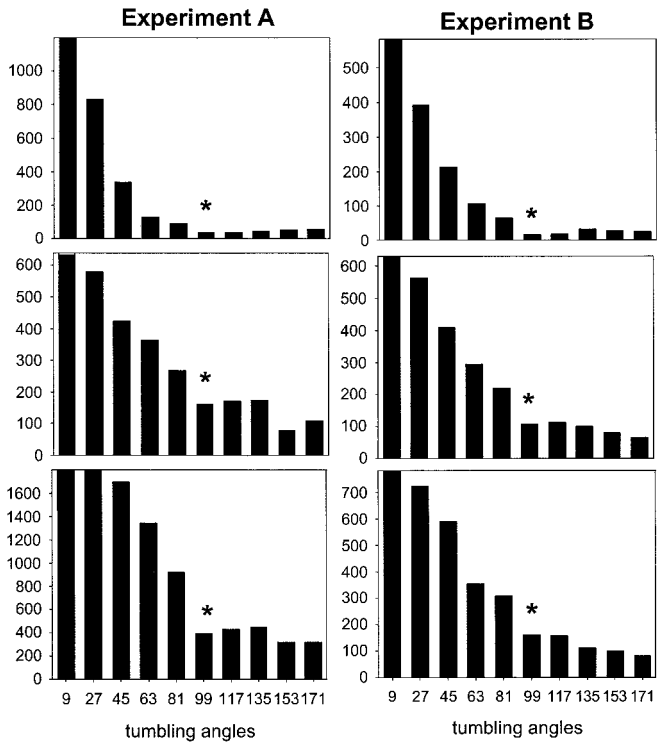

Fig. 3. Tumbling-angle histograms scaled from 0 to 180°. Ordinate is number of observations. Asterisks in histograms mark the main discontinuity observed (class 90–108°).

Flight-Time Intervals. A statistical quantity characterizing long-term random walk patterns is a flight-time interval, i.e., the period between two changes in direction (18–20). Because changes in direction were mainly due to effective tumbling angles (>100°), the flight-time distributions were obtained by computing the time spent between them. As resources decreased from high to medium concentrations, we observed a change in flight-time distributions from exponential to power law in the searching behavior of *O. marina* (25). However, no substantial change occurred in flight-time distributions between medium and low concentrations (Fig. 4). A single value for the power-law exponents of $\mu \approx 2$ was found in the two experiments. When we randomly shuffled the data that gave rise to the power laws, the long-range correlations vanished and we recovered exponential

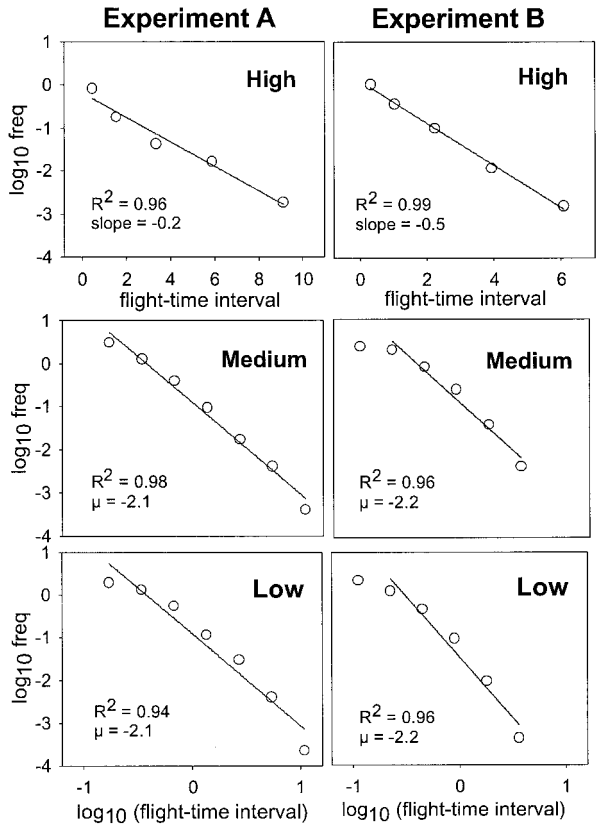

Fig. 4. Log-linear (high-resource scenario) and log–log (medium- and low-resource scenarios) plots showing the frequency distribution of flight times at each resource scenario in both experiments. We used bin widths of 2^k for the bin k and geometric midpoints of bins to plot the results. Straight lines show the least-squares fitted regressions. The first point in experiment B at medium- and low-resource scenarios was spuriously underestimated because of finite scale effects and, thus, was not fitted.

ECOLOGY

laws as expected. Moreover, crude estimations of flight times between observable reorientation leaps on the standard *O. marina* movement videotapes gave the same qualitative results and exponents for the power laws ($\mu \approx 2$), showing a good relationship between real reorientation leaps and our effective tumbling criteria (tumbling angles $>100°$).

The exponential distributions of flight times in high-resource scenarios gave rise to autoregressive random walks of order 1 (17). In these so-called Markov chains, the probability of changing direction is independent of the time walked. Positions depend on previous walk steps, but long-range correlations are not expected. Exponential laws, through the Central Limit Theorem, give rise to asymptotically Gaussian statistics (Brownian motion), and, therefore, macroscopic normal diffusions are expected, the spreading variance of organisms being proportional to time (26).

When resources are scarce, power-law distributions of flight times with scaling exponents $\mu \approx 2$ give rise to the so-called Lévy walks. Also, the points where effective tumblings occur correspond to the points visited during a Lévy flight (20). These distributions involve long-range correlations, scale-invariance, and superdiffusion phenomena (26). The probability of long travels while swimming is higher than for random walks with exponential distribution of flight times. The slight deviations from pure power laws, observed mostly when resources were scarce (i.e., low-resource scenario) could be caused by swimming interference between individuals (videotape observations). In our experiments, low prey numbers coincided with high predator concentrations (10^4 cells per ml). Interference by predators could modify the intermediate flight length regime by increasing reorientation leaps while swimming (27). In these cases, these leaps may be truly "avoidance reactions" between predators.

Discussion

The searching behavior of individuals is, at least in part, genetically encoded. Therefore, we should expect natural selection to operate on genetic variability in perceptual and motor traits underlying both behavioral decision-making and response times in the location of resources (28). Thus, the ability of an organism to optimize its encounter rate in a complex and variable environment should be honed and sharpened through evolution (29). In *O. marina*, searching behavior is adjusted in relation to resource concentration by two mechanisms controlled by flagellar movement: (*i*) at short scales, by amplitude and frequency changes in the helical path, involving continuous regulation of energy investment in the beating of transverse and longitudinal flagella; and (*ii*) at long scales, by changes in the statistics of reorientation leaps controlled by discrete strokes of the longitudinal flagellum.

Our observations suggest that the control of flagellar movement by *O. marina* admits two extreme searching behaviors in natural environments with a multiplicity of intermediate behaviors between them. When resources are readily available, *O. marina* invests more energy in movement using the longitudinal flagellum (continuous movement combined with strokes) than in movement using the transverse flagellum. Thus, the helical path follows a near-linear axis because of low amplitude and frequency of gyres. On the other hand, in medium- and low-resource scenarios, the most common in nature, *O. marina* invests more energy in movement using the transverse flagellum, which results in 3D large helicoid trajectories and in changing the statistics of the longitudinal flagellum strokes, determining the scale-invariant Lévy random searches with scaling exponent $\mu \approx 2$.

Fig. 1 shows that Lévy walks do not consist simply in adding long walks to a Brownian motion. The two types of motion differ in the whole flight-time probability distribution (i.e., short and long flight times). Lévy walks not only involve a fat-tailed flight-time probability distribution (i.e., long travels), but also a "scaling" of all flight times (i.e., no characteristic size of flight-time intervals exists). Once an observational scale is fixed, a power-law distribution of flight times (i.e., a Lévy walk) turns out to be a combination of "walk clusters" with long travels between them, giving rise to a heterogeneous multiscale-like sampling effort pattern. On the other hand, an exponential distribution of flight times (Brownian walks) gives rise to a mostly spatially homogeneous sampling effort pattern (Fig. 1). In comparing Brownian and Lévy motions with the same sampling effort, differences in the general searching pattern will appear at any scale of observation, because these differences are caused by the scaling vs. nonscaling global property of the two flight-time distributions. However, the specific consequences of the increase in the frequency of long flight times (i.e., short- vs. fat-tailed distributions) will not be observed until sufficiently large spatiotemporal scales of observation are reached. Thus, at certain scales of observation, Lévy walks may not be translated into an observational macroscopic superdiffusion of cell populations (i.e., the spreading variance of organisms being "more than" proportional to time) or into an observable decrease of individual resampling of the self-backtrails. Moreover, in *O. marina*, both effects caused by the fat tail of the Lévy walk flight-time distribution are even more difficult to observe because long travels have a strong helical component. Thus, each long time travel becomes shorter in terms of path length (i.e., linear distance traveled) than in the Brownian case (high-resource levels), where the straighter paths determine longer path lengths.

In a 3D world, and given enough time, the probability for a Brownian random walker to revisit the same point is only about 0.35, whereas in one and two dimensions this probability converges to 1 (30). Therefore, in a 3D fluid world, changes from a Brownian to a Lévy walk may not be caused by the need for the walker to avoid resampling his self-backtrails. Rather, it may be caused by the possibility of sampling a given region combining different sizes of walk clusters and long travels at different scales (i.e., a multiscale, multifractal-like pattern; refs. 31 and 32). Indeed, theoretical models have shown that even in 2D nondestructive foraging (i.e., where resampling could not be so bad to improve encounter rates) Lévy walks are better than Brownian when resources are scarce (1, 13). Conversely, they show Brownian motion not as a null model, which should be improved because of high resampling rates, but as another searching strategy that is optimal under certain conditions (i.e., high resource levels; refs. 11 and 12). Our results confirm the theoretical expectation of a switching behavior between Brownian and Lévy strategies as an optimal solution in different resource scenarios.

Then, the question turns out to be, what is the advantage to *O. marina* of performing "helical Lévy walks" instead of pure Lévy walks? Why did *O. marina* increase its helical movement component as resources decreased? Several hypotheses can be suggested, including both statistical and energetic considerations, to explain the observed change of behavior. A walker in a 3D environment, in comparison with a 2D one, not only should have less probability of resampling its own self-backtrails, but it also should have greater probability of "missing" near targets. Therefore, we suggest that larger helical paths should lead to more efficient 3D microscale explorations. Given the possibility that dinoflagellates also use their chemosensory abilities (33) to find their prey, the radius and the pitch of the helicoid (34) should be larger than the nearby space covered by organisms' sensorial structures to have an efficient search. Larger helical paths may also increase the long-term Lévy walk statistical efficiency of encounters by avoiding midterm curvilinear biases of long travels (14, 35). Moreover, while following large helicoids, *O. marina* invests more energy in movement by using the transverse flagellum than the longitudinal one. Experimental

reactivation of isolated and permeabilized flagella of *O. marina* suggests that energetic requirements for the two flagella are similar (15). Therefore, if some energetic advantage is involved in performing larger helical paths, it should be related not to the differential use of flagella but to other factors.

A good 3D search should involve both short- and long-term efficient searching strategies. Optimal long-term searching strategies are independent of the dimension of the foraging space (11, 12, 36), but this independence may not hold for the short-term component of a searching process that may change with the number of dimensions used in the exploration. The possibility that, in a 3D environment, the incorporation of long helical paths (i.e., as a short-scale searching strategy) improves the statistics of encounters by decreasing the probability of "missing" near targets and/or by avoiding midterm curvilinear biases, or whether it reduces some energetic costs, remains an open question that needs further consideration.

In conclusion, we suggest that the chance of finding food in 3D environments depends not only on the *path lengths* (i.e., linear distances traveled) but also on the *whole shape* of the walk. Long path lengths mainly explain the avoidance of resampling backtrails but, as we have argued, is not necessarily the key aspect for optimizing encounters in a 3D exploration. Efficient sampling in a low-Reynolds number 3D environment without cues may be based not on rapidly avoiding regions with scarce resources but on exploring the whole environment at the largest range of possible scales while maintaining an efficient local exploration (whether energetic or statistical) of the 3D environment. Based on these sampling requirements, we suggest that helical Lévy walks optimize random searching (i.e., number of encounters with prey) in 3D environments with low prey densities. Helical Lévy walks may be as widely spread among dinoflagellates (35) and other microzooplankters (34) as pure fractal (37) and multifractal (38) random walks are among macrozooplankters. However, a variety of specific motion mechanisms could be involved in this type of random searching motion.

Further, our results are consistent with the hypothesis that the exponent $\mu_{opt} = 2$ may be universal, i.e., independent of the dimension of the foraging space (11, 12, 36) and robust with respect to short-scale effects, including effects on the organisms' behavior and physiology (27, 39, 40). The example given here demonstrates the usefulness of random search theory for providing a more realistic view of ecological interactions. We hope our case study will encourage ecologists to reexamine the hitherto traditionally applied "mean field" assumption in ecological theory.

F.P. and C.M. designed and performed the experiments, and F.P. prepared the procedure for image analyses. The methods and criteria for data analyses were established by S.P. and F.B. (with a larger contribution from S.P.) and applied by F.B.; the text was written by F.B. and J.C. with input from all coauthors. We thank M. Castaño, A. Lorente, and J. Piera for help at different stages of this work and for discussions, and two anonymous reviewers for comments on the manuscript. D. Balayla revised the English typescript. F.B. was the recipient of a Comissió Interdepartamental de Recerca i Innovació Tecnològica fellowship (1997FI 00296 UB APMARN). F.P. received a European Union postdoctoral grant (ERBFMBICT950195) and acknowledges the support of the European Union project Nutrient Dynamics Mediated through Turbulence and Plankton Interactions (EVK3-CT-2000-0022). This article is European Land Ocean Interaction Studies Contribution 402/40.

1. Viswanathan, G. M., Budyrev, S. V., Havlin, S., da Luz, M. G. E., Raposo, E. P. & Stanley, H. E. (1999) *Nature* **401,** 911–914.
2. Levandowsky, M., Klafter, J. & White, B. S. (1988) *J. Protozool.* **35,** 243–246.
3. Levandowsky, M., Klafter, J. & White, B. S. (1988) *Bull. Mar. Sci.* **43,** 758–763.
4. Klafter, J., White, B. S. & Levandowsky, M. (1989) in *Biological Motion*, eds. Hoffmann, G. & Alt, W. (Springer, Heidelberg), pp. 281–296.
5. Heinrich, B. (1979) *Oecologia* **40,** 235–245.
6. Levandowsky, M., White, B. S. & Shuster, F. (1997) *Acta Protozool.* **36,** 237–248.
7. Cole, B. J. (1995) *Anim. Behav.* **50,** 1317–1324.
8. Focardi, S., Marcellini, P. & Montanaro, P. (1996) *J. Anim. Ecol.* **65,** 606–620.
9. Viswanathan, G. M., Afanasyev, V., Budyrev, S. V., Murphy, E. J., Prince, P. A. & Stanley, H. E. (1996) *Nature* **381,** 413–415.
10. Atkinson, R. P. D., Rhodes, C. J., Macdonald, D. W. & Anderson, R. M. (2002) *Oikos* **98,** 134–140.
11. Bartumeus, F., Catalan, J., Fulco, U. L., Lyra, M. L. & Viswanathan, G. M. (2002) *Phys. Rev. Lett.* **88,** 097901–097904.
12. Bartumeus, F., Catalan, J., Fulco, U. L., Lyra, M. L. & Viswanathan, G. M. (2002) *Phys. Rev. Lett.* **89,** 109902(E).
13. Viswanathan, G. M., Bartumeus, F., Buldyrev, S. V., Catalan, J., Fulco, U. L., Havlin, S., da Luz, M. G. E., Lyra, M. L., Raposo, E. P. & Stanley, H. E. (2002) *Physica A* **314,** 208–213.
14. Levandowsky, M. & Kaneta, P. J. (1987) in *The Biology of Dinoflagellates*, ed. Taylor, F. J. R. (Blackwell Scientific, Oxford), pp. 360–398.
15. Cosson, J., Cachon, M., Cachon, J. & Cosson, M. P. (1988) *Biol. Cell* **63,** 117–126.
16. Cachon, M., Cosson, J., Cosson, M. P., Huitorel, P. & Cachon, J. (1988) *Biol. Cell* **63,** 159–168.
17. Chatfield, C. (1984) *The Analysis of Time Series: An Introduction* (Chapman & Hall, London), 3rd Ed.
18. Mandelbrot, B. B. (1982) *The Fractal Geometry of Nature* (Freeman, San Francisco).
19. Shlesinger, M. F., Zaslavsky, G. & Klafter, J. (1993) *Nature* **363,** 31–37.
20. Shlesinger, M. F., Zaslavsky, G. & Frisch, U., eds. (1995) *Lévy Flights and Related Topics in Physics* (Springer, Berlin).
21. Voss, R. F. (1989) *Physica D* **38,** 362–371.
22. Middleton, G. V., Plotnick, R. E. & Rubin, D. M. (1995) *Nonlinear Dynamics and Fractals: New Numerical Techniques for Sedimentary Data* (Society for Sedimentary Geology, Tulsa, OK).
23. Berg, H. C. (1983) *Random Walks in Biology* (Princeton Univ. Press, Princeton), pp. 75–94.
24. Crenshaw, H. C., Ciampaglio, C. N. & McHenry, M. (2000) *J. Exp. Biol.* **203,** 961–982.
25. Pueyo, S. (2003) *Irreversibility and Criticality in the Biosphere* (Publicacions Universitat de Barcelona, Barcelona), in press.
26. Weeks, E. R. & Swinney, H. L. (1998) *Phys. Rev. E* **57,** 4915–4920.
27. da Luz, M. G. E., Buldyrev, S. V., Havlin, S., Raposo, E. P., Stanley, H. E. & Viswanathan, G. M. (2001) *Physica A* **295,** 89–92.
28. Bell, W. J. (1991) *Searching Behaviour: The Behavioural Ecology of Finding Resources* (Chapman & Hall, London).
29. Catalan, J. (1999) *Jpn. J. Limnol.* **60,** 469–494.
30. Feller, W. (1968) *An Introduction to Probability Theory and Its Applications* (Wiley, New York), Vol. 1, pp. 359–362.
31. Nakao, H. (2000) *Phys. Lett. A* **266,** 282–289.
32. Jaffard, S. (1999) *Probab. Theory Relat. Fields* **114,** 207–227.
33. Hauser, D. C. R., Levandowsky, M. & Glassgold, J. M. (1975) *Science* **190,** 285–286.
34. Ricci, N. (1996) in *Ciliates: Cells as Organisms*, eds. Hausmann, K. & Bradbury, P. C. (Gustav Fisher, Stuttgart), pp. 403–416.
35. Kamykowski, D., Reed, R. E. & Kirkpatrick, G. J. (1992) *Mar. Biol. (Berlin)* **113,** 319–328.
36. Viswanathan, G. M., Afanasyev, V., Budyrev, S. V., Havlin, S., da Luz, M. G. E., Raposo, E. P. & Stanley, H. E. (2001) *Physica A* **295,** 85–88.
37. Coughlin, D. J., Strickler, J. R. & Sanderson, B. (1992) *Anim. Behav.* **44,** 427–440.
38. Schmitt, F. G. & Seuront, L. (2001) *Physica A* **301,** 375–396.
39. Peters, F. (1994) *Limnol. Oceanogr.* **39,** 195–206.
40. Yamazaki, A. K. & Kamykowski, D. (2000) *Ecol. Modell.* **134,** 59–72.